THE TECHNOLOGY HERITAGE OF THE RELATIVITY MISSION, GRAVITY PROBE B

SAPS BUCHMAN, FRANCIS EVERITT, BRAD PARKINSON, J.P. TURNEAURE, D. DEBRA, D. BARDAS, W. BENCZE, R. BRUMLEY, D. GILL, G. GREEN, G. GUTT, J. GWO, J. KASDIN, M. KEISER, J. LIPA, J. LOCKHART, J. MESTER, B. MUHLFELDER, M. TABER, S. WANG, Y. XIAO, and P. ZHOU
W. W. Hansen Experimental Physics Laboratory, Stanford University, Stanford, CA 94305, U.S.A.

The Relativity Mission program has developed a rich heritage of technologies applicable to future precision experiments in space. We describe the principal systems with technology relevant to the STEP and LISA missions.

1 Introduction

The Relativity Mission, also known as Gravity Probe B (GP-B), is first in a series of challenging space science experiment. Taking advantage of the space environment to reduce gravitational disturbances, these missions are designed to measure relativistic effects with accuracies of four to seven orders of magnitude better than those achievable on the ground. State of the art technology must be developed to meet the challenge of attaining the experimental accuracy and to compensate for the demanding space environment.

GP-B [1] is a test of the rotational effects of gravity designed to measure the geodetic and frame dragging relativistic rotational precessions. The local frame of reference in a 650 km polar orbit, determined by high precision gyroscopes, is compared with the fixed frame of reference of distant stars, determined by a telescope. Figure 1 is a schematic representation of the GP-B experimental concept.

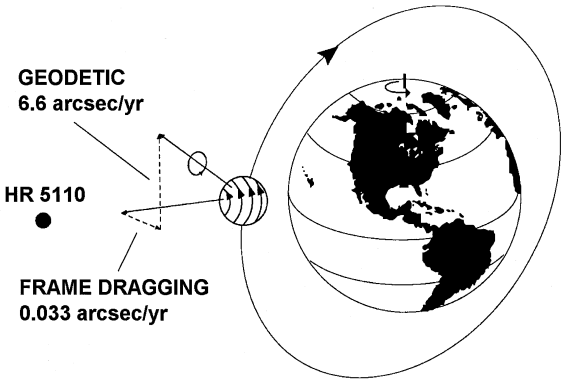

Figure 1: GP-B experimental concept

In General Relativity the magnitudes of the geodetic and frame dragging precessions are 6.6 $arcsec/yr$ and 0.033 $arcsec/yr$, to be measured in the Relativity Mission with an accuracy of 0.3 $marcsec/yr$ or better. STEP and LISA, two major

space tests of gravitational theories, utilize technologies similar to those developed for GP-B.

STEP, the Space Test of the Equivalence Principle [2], is designed to test the equivalence of the inertial and gravitational masses to 10^{-17} , an improvement of six orders of magnitude below the present results obtained by ground based experiments. Differential cryogenic accelerometers, each containing two cylindrically symmetric and concentric test masses made of different materials, are placed in a drag free trajectory, in Earth orbit, at 550 km altitude and 97 degrees inclination. Linear bearings and sensing circuits constrain the relative motion of the two test masses two a one dimensional motion. Violation of the equivalence principle would result in a differential acceleration of the test masses, and consequently their relative displacement at orbital frequency. Figure 2 shows the STEP experiment principle.

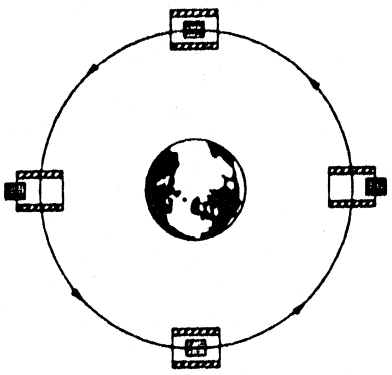

Figure 2: STEP experiment

LISA, the Laser Interferometer Space Antenna [3], is a Michelson interferometer placed in space and designed to detect gravitational waves. Three identical spacecraft, located at the vertexes of an equilateral triangle of 5×10^6 km on each side, define the two primary arms and the redundant arm of the interferometer. The constellation is placed in a heliocentric orbit, 1 AU from the Sun, and 20 degrees behind the Earth, while the three spacecraft move relative to each other in a circular orbit inclined at 60 degrees to the ecliptic. Each spacecraft contains two drag free reference mirrors which define the interferometer cavity and two 30 cm aperture telescopes. The telescopes point at the neighboring spacecraft and are used for transmitting and receiving the phase-locked 1064 nm Nd:YAG laser beams. The operational temperature of the drag free mirrors is between 200 K and 250 K. Figure 3 represents schematically the LISA configuration. LISA's mission objective is the detection of gravitational radiation in the frequency range of 10^{-4} Hz to 10^{-1} Hz, with a strain sensitivity of $4 \times 10^{-21}/\sqrt{Hz}$ at 10^{-3} Hz. The residual disturbance forces on the drag free reference mirrors must be limited to 10^{-15} m/s^2 in the measurement frequency band.

Use of GP-B heritage for following experiments will optimize the utilization of technology resources, allowing the faster, better, cheaper approach to space science.

This heritage includes scientific and technological experience, as well as flight operational experience and flight data available after the year 2000. With their large number of common technologies, STEP and LISA appear ideally suited for such technology re-utilization. The following sections describe a number of GP-B developed systems and technologies whose heritage has direct applications for future missions. It is important to note that all these very precise systems are capable of withstanding the highly demanding space and launch environments.

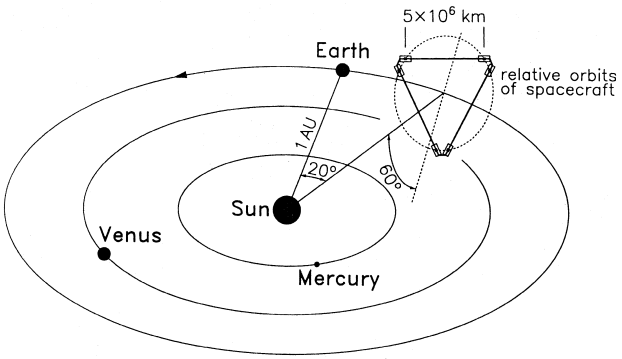

Figure 3: LISA experimental concept

2 Gyroscopes and drag free sensors

Four high precision cryogenic electrostatically suspended gyroscopes, with a maximum allowable drift rate of 0.3 $marcsec/yr$, are used in GP-B to determine the inertial reference frame in the vicinity of Earth. Residual torques are reduced to a minimum by compensating for the drag on the satellite [4] and by carefully controlling the sphericity of the gyroscope and its housing. In order to ensure space functionality, the gyroscopes are capable of operation on the ground. The technology aimed at ground testing and ground simulation of space operations has been fully developed. Four gyroscopes are fabricated, two of fused quartz and two of single crystal silicon. The density uniformity of the quartz is measured to a few parts in 10^8 by an interferometric technique using a cube of material immersed in index matching fluid.[5] Figure 4 shows an exploded view of a gyroscope.

Gyroscope rotors are polished into accurate spheres using laps arranged in a tetrahedral configuration, and measured using a precision mechanical spindle with an LVDT transducer. A measurement over 17 great circles of each rotor insures good mapping of the spherical surface. The peak to valley deviation of the rotor surface from the best fit sphere is about 10^{-6} with respect to the 1.9 cm gyroscope radius, or about 20 nm. A film of niobium 1.25 μm thick is sputtered onto the rotors in 26 symmetric patches, achieving a peak-to-valley uniformity of better than 2%, or about 25 nm.[6] The very good spherical surface of the gyroscope rotors reduces the torques caused by the electrostatic suspension.

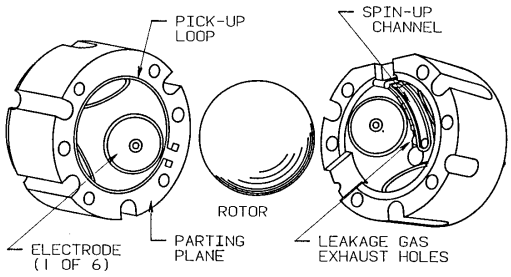

Figure 4: Schematic view of gyroscope

The spherical cavity of the gyroscope housing is polished using a "tumble lapping" technique, whereby the two housing hemispheres are closed around a heavy lap in the shape of a spherical cap, and the whole assembly is randomly tumbled. A judicious combination of lap weight, tumbling speed, and polishing compound insures that the lap remains in within 40 degrees from the bottom of the cavity during the tumble lapping operation. The peak to valley sphericity of the approximately 1.9 cm radius cavities thus produced is equal to or less than 150 nm. Titanium copper multi-layer coatings are then sputtered onto the electrode areas, providing the necessary electrical and thermal conductivity. [7] In order to withstand launch loads the gyroscope rotors are caged with a piston activated by a liquid helium pressurized set of diaphragms.

The unsupported gyroscope, which is also used as the drag free sensor, does not need electrostatic support, thus eliminating the largest disturbance precession. The expected drift rate of the electrostatically supported gyroscopes is about 0.15 $marcsec/yr$, while the expected drift rate of the gyroscope utilized as a drag free sensor is about 0.02 $marcsec/yr$. Functioning as an accelerometer, the GP-B gyroscopes are designed to measure $2 \times 10^{-12}\ ms^{-2}/\sqrt{Hz}$ at the satellite roll frequency of a few millihertz. 100,000 hours of ground testing of the gyroscopes has demonstrated a performance consistent with the Relativity Mission requirements, indicating that the performance of the unsupported gyroscope [8] will allow the measurement of γ to better than one part in 10^4. Studies evaluating the performance of the GP-B gyroscopes as accelerometers for future space experiments show that very good accelerometer performance can be achieved by removing the stringent GP-B gyroscope functionality requirements placed upon these devices.

3 SQUID technology for space applications

The gyroscope readout system for GP-B is based on the London moment, whereby a rotating superconductor produces throughout its volume a magnetic field aligned with the spin axis. For the spherical gyroscope the resulting magnetic dipole moment represents the angular momentum direction to be measured in the experiment.

Figure 5 is a simplified schematic of the London moment readout concept. Experiments conducted at GP-B have demonstrated that the London moment is the ground state of a superconducting rotating sphere. [9] The same London magnetic

dipole is achieved independently of the thermal history of the process, that is cooling through the superconducting transition followed by spinning, or cooling after spinning. An ultra low noise dc SQUID system has been developed for GP-B, incorporating state of the art shielding and filtering techniques, and optimized for work in the presence of the disturbances caused by the gyroscope suspension. At the 5 mHz detection frequency, the noise performance of the read-out in the flight system is about 8×10^{-29} J/Hz. This is equivalent to a resolution of 1 $marcsec$ in an integration time of eight hours, or about 20% better than the GP-B requirements.

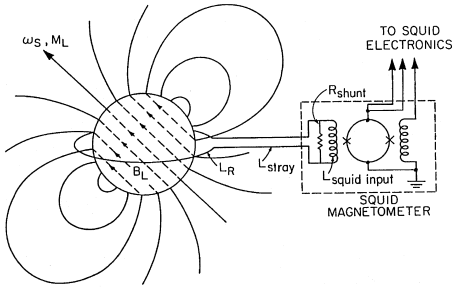

Figure 5: London moment readout system schematic

4 Cryogenic telescope

In order to provide the reference to the fixed frame of the distant stars, GP-B has developed a cryogenic Cassegrainian telescope with a focal length of 381 cm and an aperture of 14.4 cm. The telescope and the quartz block mounting the four gyroscopes are bonded and maintained at cryogenic temperatures, thus ensuring the ultra low mechanical drift between these instruments. A novel bonding technique using potassium hydroxide has been developed for use in all optical bonds of the telescope and of the other components of the science instrument. Bond strength achieved by this method is in excess of 3×10^7 Pa, with the interface thickness limited by the surface flatness of the components to be joined.

Thermal expansion is a serious concern for cryogenic optical instruments which have to be built and pre-calibrated at room temperature. In order to minimize thermal distortion, the fused quartz used for the main GP-B telescope components and the quartz block is from a single specially fabricated quartz boule. Therefore these components have matched ultra low coefficients of thermal expansion: $\Delta CTE \leq 10^{-9}$.

The telescope detection system uses photodiodes with JFET amplifiers functioning at 70 K, resulting in a pointing noise for the instrument of 10 $marcsec/\sqrt{Hz}$. In order to minimize the thermal load to the 2.2 K helium bath a thermal platform with very low thermal conductivity has been developed for the detector assembly. Repeated accurate mounting on the telescope of the package containing the detector assembly is made possible by a precision mounting fixture.

A set of four optical windows, one sapphire and three quartz, allow the light

from the star to penetrate to the cryogenic region of the experiment. The four main requirements for the optical window system pertain to optical transmission, EMI rejection, optical distortion, and maintenance of the instrument vacuum. The outer window mounting seal maintains the $10^{-9}\ Pa$ ultra high vacuum, of the GP-B experiment. Special coatings ensure both an optical transmission of at least 70% in the 400 nm to 1000 nm band, and an EMI rejection in excess of 50 dB. Finally, high quality sapphire and quartz material, combined with special polishing and mechanical mounting techniques, minimize optical distortions caused by thermal gradients.

5 Magnetic shielding

The London moment based readout requires shielding from external ac magnetic fields by 10^{12}, while a dc field of less than $10^{-11}\ T$ is needed to insure low trapped flux in the gyroscopes. This is achieved by using a system of superconducting magnetic shields, in conjunction with controlling the magnetic properties of the probe materials. A ferromagnetic shield provides a $10^{-6}\ T$ magnetic field region within which the main field reduction is attained by the expansions of superconducting lead foil cylinders. The foil cylinder, folded to minimize the cross-sectional area, is cooled through its superconducting transition temperature. Cooling rates are controlled in order to minimize thermal gradient induced currents. Once the lead cylinder is superconducting, it is mechanically unfolded to its maximum diameter. This operation reduces the magnetic flux in the cylinder by roughly the ratio of the folded to the expanded cross-sectional areas, a factor of about 20 in practice.[10] Figure 6 represents schematically the expansion process. The process is repeated with additional lead cylinders being expanded one at a time inside the reduced field produced by the previous expansions. The lowest magnetic field values reached are about $5 \times 10^{-12}\ T$; with further reduction prevented by thermoelectric effects in the lead foil.

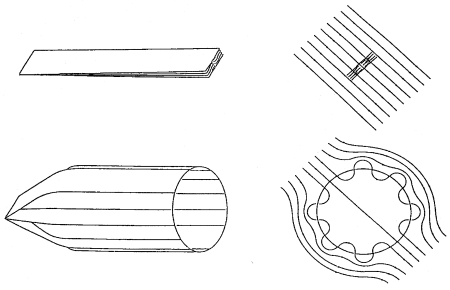

Figure 6: Lead cylinder expansion

The ferromagnetic shield and lead foil superconducting cylinder provide an ac shielding factor of about 10^9, while a superconducting niobium cylinder surrounding the gyroscope brings the final shielding factor to 10^{12}. Finally, the superconducting gyroscope rotor shields the readout loop from external fields by an additional factor

of ten. Integrated system tests have confirmed the performance of these magnetic shielding techniques.

6 Precise ultra stable structures

The main components of the GP-B science instrument, telescope and quartz block with four gyroscopes, must maintain highly demanding mechanical stabilities with respect to each other in order to achieve the required measurement accuracy. Advanced material science, machining, and mechanical mounting techniques have been developed to achieve these goals. All quartz interfaces are precision machined and optically polished to allow bonding. Figure 7 is a schematic representation of the cryogenic probe.

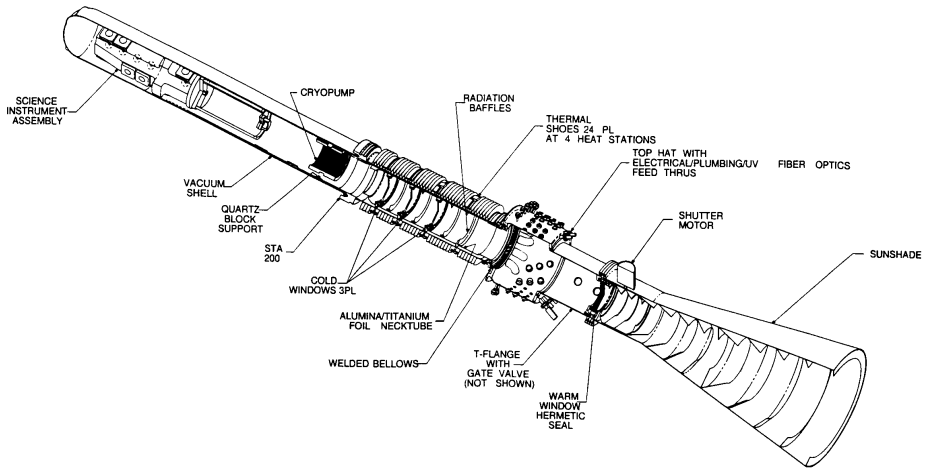

Figure 7: Schematic representation of the cryogenic probe

The telescope and the gyroscopes are mounted to the quartz block by potassium hydroxide bonding and special mechanical mounts ensuring an angular stability in inertial space between the readout loops of the gyroscopes and the telescope axis of better than 0.1 $marcsec/yr$, and an alignment better than 5 $arcsec$. In order to minimize centrifugal forces on the gyroscopes, caused by satellite roll, all four gyroscope centers are aligned to the roll axis to better than 0.1 mm, while their spacing tolerance along the telescope axis is less than 1 mm.

The science instrument is mounted to the cryogenic probe via a quartz to aluminium interface which must meet thermal conductivity and mechanical stress requirements. Special mechanical fasteners and molybdenum thermal shoes have been developed to meet these requirements, while at the same time being able to withstand the launch loads without inducing excessive stress in the quartz. Assembled at room temperature for use in superfluid helium, the entire probe science instrument structure is designed for full functionality over the 350 K to 2 K thermal range.

7 Cryogenic technology for space

Cryogenic temperatures for the GP-B experiment are maintained by the 1,500 liter capacity, 18 months lifetime superfluid helium flight dewar. Figure 8 is a schematic representation of the flight dewar. A number of unique technologies have been developed to minimize the heat input into the helium bath, and thus maximize mission lifetime.

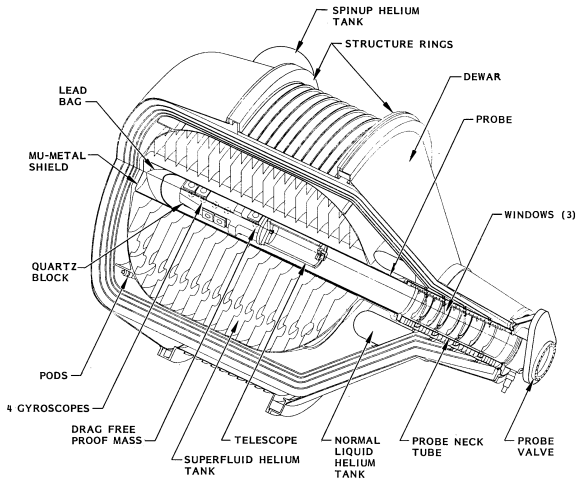

Figure 8: Schematic representation of the flight dewar

PODS [13], passive orbital disconnect struts, are mechanical devices which support the helium tank with respect to the outer dewar shell under Earth gravity and launch loads, while passively breaking this thermal link in orbit. To minimize thermal radiation down their center, the emergency vents are built of folded pliable material. These deployable vent tubes will be inflated open by the gas escaping during an emergency venting. A normal helium guard tank, placed at the neck of the dewar, makes it possible to maintain the main tank full for extended periods on the launch pad. The helium in the guard tank will be drained just prior to launch. Helium levels will be periodically ascertained in orbit by the use of a heat pulse method, whereby the temperature increase caused by a calibrated heat input is measured.

A 'porous plug' maintains the helium bath at superfluid temperatures. This plug consists of a calibrated superfluid leak, ensuring well defined high gas flow rates over a range of temperatures, while inhibiting superfluid breakthrough. The venting helium is utilized as propellant by the proportional thrusters which control the attitude, roll, and drag free functions of the spacecraft. Models of the dynamics of a superfluid in low gravity have been used to develop a set of baffles internal to the main helium tank. These baffles restrain the movement and maintain the symmetry of the decreasing volume of liquid helium during the mission. The completed GP-B flight dewar has met all thermal requirements in ground testing.

8 Mitigation of cosmic radiation effects

Of major concern for high accuracy experiments with floating test masses are the effects of cosmic radiation caused by charged particles from the Earth's radiation belts, solar flares, and other galactic sources. [11] For the GP-B gyroscopes these effects are charging, heating, momentum transfer, and the trapped flux motion in the gyroscope coating. Note that only the protons affect the gyroscopes, as the shielding provided by the spacecraft stops most electrons. GP-B has developed mitigation techniques for these problems which have direct bearing upon the STEP and LISA experiments.

A radiation shield of 10 g/cm^{-2} was added to the internal structure of the dewar to reduce heating and charging during solar flares, resulting in a total shielding for the gyroscopes of 20 g/cm^{-2} aluminium equivalent. Gyroscope rotors are mechanically isolated systems spinning in ultrahigh vacuum, thus making it necessary to use non-contact methods for charge control and to rely on thermal radiation for cooling. Torque and acceleration considerations, limit the rotor charge to 15 pC, or equivalently to a 15 mV potential (1 nF rotor capacitance). The total charge accumulation over the 1.5 year mission is about 600 pC, thus making it necessary to use active charge control.

The rotor charge is measured using a using a force modulation method, in which excitation voltages of about 20 mV peak-to-peak amplitude are applied 180 degrees out-of-phase to two opposite electrodes. This technique achieves an accuracy of better than 4 mV for an integration time of 100 s, making it suitable for use in the GP-B mission. The force modulation method is insensitive to gyroscope miscentering and is independent of the ambient acceleration. UV photoemission is the method used by GP-B to generate the electrons used for charge control. [12] The rotor and the charge control electrode are illuminated with UV light, and electrons are generated by photoemission from both these surfaces. The direction of the charge flow to the rotor is controlled by biasing the charge control electrode to ± 3 V.

The gyroscope surface is a sputtered thin film of niobium, while the charge control electrode surface is electroplated gold. Experimental considerations pose additional constraints on the hardware near the gyroscope: low remnant magnetization, very high standards of cleanliness, and compatibility with the 2.5 K GP-B experimental temperature. An alternate method of charge control, using field emission cathodes, has demonstrated very good results, and might be the technique of choice for LISA and STEP.

At the operating pressure, 10^{-9} Pa at 2.5 K, thermal radiation is the main cooling mechanism for the rotor. The rotor temperature will be about 3.6 K, (1.1 K above the gyroscope housing temperature), for 1 nW heat input and the measured thermal emissivity of about 3%. A three day major solar flare will raise the rotor temperature to about 5.5 K, safely below its 9 K superconducting transition. Note that without the radiation shield the equivalent temperatures would be respectively 4.1 K and 10.0 K. Calculations and computer simulations show that torques and trapped flux motion induced by protons cause negligible errors.

Ground testing has shown that charge management, using measurement by force

modulation and electrons generated by ultraviolet photoemission, is the solution for the GP-B gyroscope charging problem. We conclude that the GP-B gyroscope performance will not be degraded by cosmic radiation.

9 Flight electronics for high precision experiments

The GP-B payload electronics systems are the gyroscope suspension, the SQUID readout, and the telescope readout. All these systems must meet their own demanding requirements, while at the same time maintain compatibility with the functionality of the other system.

The electrostatic gyroscope positioning and suspension electronics was developed as a dual digital and analog system. An R6000 digital processor allows for maximum flexibility and the option of uploading new software to orbit, while the analog backup ensures maximum reliability in the space debris and radiation environment. Support for the ground testing capability of the gyroscopes has resulted in the system having full functionality over the range of 10^{-8} g to 1 g. The electrostatic suspension also supports the accelerometer function of the gyroscope in the drag free position, with a performance of 2×10^{-12} $ms^{-2}/\sqrt{Hz}$. Additional functions supported by the gyroscope suspension system are charge measurement and control, gyroscope spinup, and spin axis alignment. Preliminary studies show that the accelerometer performance of this electrostatic system can be significantly enhanced by removing the GP-B gyroscope functionality requirements, thus making it a candidate for use in future missions.

The dc SQUID readout system is designed for the ultra low noise measurement of the London magnetic dipole variations in the relatively noisy environment created by the gyroscope suspension systems. Sophisticated shielding and filtering techniques have been developed for both the SQUID sensor and its cryogenic cables. The telescope readout provides accurate pointing data for the space vehicle by using photodiode generated currents of about 10^{-14} A.

Grounding and shielding methods have been developed to meet the required electromagnetic interference environment for the low noise measurement, while in order to further reduce interference, the entire spacecraft uses a synchronized timing scheme. The electronics designs have been implemented using radiation hardened components with low sensitivity to single event upsets and latchups, a number of which were custom designed and space qualified for GP-B. Finally, gyroscope and SQUID system hardware simulators have been developed to ensure full testability of the electronic systems.

10 Spacecraft for complex space experiments

The GP-B spacecraft is tailored to support the high accuracy cryogenic experiment. Using the helium proportional thrusters developed by this program, the spacecraft systems control drag free navigation, attitude, and roll. Star trackers are used to sense roll rate, while rate gyroscopes sense the orientation of the spacecraft when the guide star is occulted by the Earth. The star trackers and rate gyroscopes are

mounted on precision instrumentation platforms connected to a graphite ring in the dewar structure, ensuring a stable mechanical reference to the science instrument.

The space environment is monitored by particle detectors and magnetometers whose output will allow direct correlation of the science data with anomalous radiation or magnetic events. A global positioning system, GPS, ensures accurate orbit insertion and trim. Orbit parameters will be continuously monitored by GPS and by laser ranging to a set of retro-reflectors mounted on the spacecraft. All spacecraft systems are designed to meet the high reliability appropriate for this type of experiment. Figure 9 is a schematic representation of the GP-B satellite.

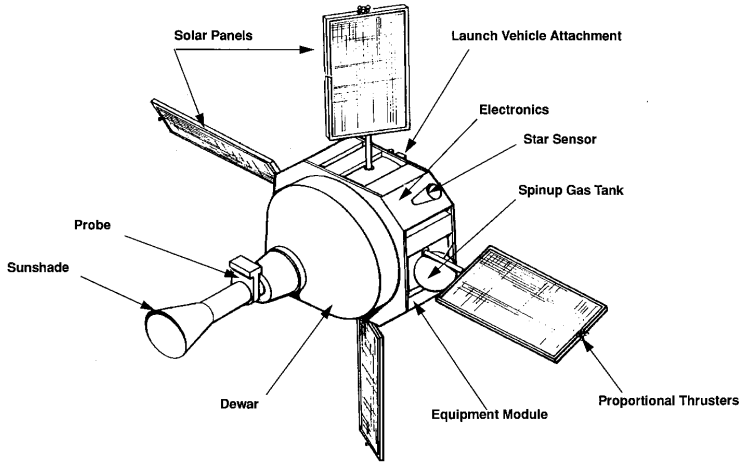

Figure 9: Schematic representation of the GP-B satellite

11 Conclusions

GP-B has developed and implemented a large number of technologies with direct application to future precision space experiment in general, and to the STEP and LISA missions in particular. The program has also perfected the incremental prototyping approach to hardware and integrated testing, thus ensuring the successful development of the complex instruments needed for this class of experiments.

A highly elaborate operational time line has been developed for the mission, including initial calibrations and setup, science operations, and post mission calibrations. Space operations for GP-B are planned to be controlled locally, from the development site, by making use of the Stanford University radiotelescope antenna. Operational experience and data from the Relativity Mission will be a major component of this program's heritage.

Acknowledgments

This work was supported by NASA contract NAS8-39225.

References

1. J. P. Turneaure, C. W. F. Everitt, B. W. Parkinson, *Advances in Space Research* **9**, 29 (1989).
2. P.W. Worden Jr.in *A Cryogenic Test of the Equivalence Principle*, (PhD thesis, Stanford University, Stanford, California 1974).
3. D. Hils, P.L. Bender, and R.F. Webbink, *Astrophys. J.* **360**, 75 (1990).
4. D.B. DeBra in *DISCOS Description*, (Private communication, Stanford University, Stanford, California 1970).
5. J. M. DeFreitas in *Interferometric characterization of Refractive Index Variations in Vitreous Silica*, (PhD thesis, University of Aberdeen, Aberdeen, UK 1994).
6. D. Gill, P. Peters, C. Sisk, *Proceedings of the 15th International Conference on Metallurgical Coatings*, (Elsevier Sequoia, 1988).
7. P. Zhou, S. Buchman, K. Davis, C. Gray, and J.P. Turneaure, *Surface and Coatings Technology* **76-77**, 516 (1995).
8. C. W. F. Everitt and S. Buchman in *Particle Astrophysics, Atomic Physics, and Gravitation*, (Editions Frontieres, Cedex-France, 1994).
9. Y. Xiao *et al.*, *Physica B* **194-196**, 65 (1994).
10. M. Taber *et al.*, *Adv. Cryogenic Eng.* **39**, 161 (1993).
11. Y. Jafrey, T.J. Sumner, and S. Buchman, *Classical and Quantum Gravity* **13**, A97 (1996).
12. Saps Buchman, T. Quinn, G.M. Keiser, D. Gill and T.J. Sumner, *Rev. Sci. Instrum.* **66**, 120 (1995).
13. I. Spradley and R.T. Parmley, *Adv. Cryogenic Eng.* **33**, (1987).